CONF-860421--16

CORROSION OF Fe-Cr-Mn ALLOYS IN THERMALLY CONVECTIVE LITHIUM*

P. F. Tortorelli and J. H. DeVan

Oak Ridge National Laboratory
Oak Ridge, Tennessee 37831

MASTER

Abstract

A series of austenitic Fe-Cr-Mn steels was exposed to circulating lithium at temperatures up to 500°C. Two groups of the alloys, which contained 12 to 30 wt % Mn and 2 to 20 wt % Cr, were sequentially exposed for periods greater than 3000 h in a type 316 stainless steel thermal convection loop. Mass transfer of manganese caused very large weight losses from the steels containing 30 wt % Mn. However, the actual magnitude of corrosion losses for alloys containing 12 to 20 wt % Mn was difficult to establish due to competing surface reactions involving chromium.

---

*Research sponsored by the Office of Fusion Energy, U.S. Department of Energy under contract DE-AC05-84OR21400 with the Martin Marietta Energy Systems, Inc.

By acceptance of this article, the publisher or recipient acknowledges the U.S. Government's right to retain a nonexclusive, royalty-free license in and to any copyright covering the article.

CONF-860421--16

DE86 009153

DISCLAIMER

This report was prepared as an account of work sponsored by an agency of the United States Government. Neither the United States Government nor any agency thereof, nor any of their employees, makes any warranty, express or implied, or assumes any legal liability or responsibility for the accuracy, completeness, or usefulness of any information, apparatus, product, or process disclosed, or represents that its use would not infringe privately owned rights. Reference herein to any specific commercial product, process, or service by trade name, trademark, manufacturer, or otherwise does not necessarily constitute or imply its endorsement, recommendation, or favoring by the United States Government or any agency thereof. The views and opinions of authors expressed herein do not necessarily state or reflect those of the United States Government or any agency thereof.

DISTRIBUTION OF THIS DOCUMENT IS UNLIMITED

CORROSION OF Fe-Cr-Mn ALLOYS IN THERMALLY CONVECTIVE LITHIUM*

P. F. Tortorelli and J. H. DeVan

Oak Ridge National Laboratory
Oak Ridge, Tennessee 37831

Introduction

Austenitic Fe-Cr-Mn alloys can serve as an alternative to the traditional Fe-Cr-Ni stainless steels. Such alloys are of particular interest to fusion technology because of their substantially lower residual radioactivity compared to that for the standard nickel-containing austenitic stainless steels [1]. However, for fusion applications, the Fe-Cr-Mn steels must first exhibit resistance to both radiation damage and corrosion. Of particular interest is the corrosion of Fe-Cr-Mn alloys by molten lithium, which is a possible coolant and/or tritium-breeding fluid for D-T fusion reactors. To date, studies of the corrosion of these alloys by molten lithium were conducted under static conditions [2–6]. In this paper, qualitative results on the corrosion of a number of Fe-Cr-Mn alloys exposed to thermally convective lithium are presented and compared to the earlier work in a static lithium environment.

Experimental procedures

Fe-Cr-Mn steel specimens were exposed to lithium in a type 316 stainless steel thermal convection loop that allowed removal and insertion of specimens without discontinuing the lithium flow [7] and had previously operated for many thousands of hours with specimens of other alloys. The lithium density gradient caused by the imposition of a temperature difference of 150°C across the loop resulted in an average flow rate of

*Research sponsored by the Office of Fusion Energy, U.S. Department of Energy under contract DE-AC05-840R21400 with the Martin Marietta Energy Systems, Inc.

approximately 25 mm/s. Such a slow flow rate would be characteristic of lithium being used as a semistagnant tritium breeding fluid. Typical impurity concentrations of the purified lithium were 30 to 100 wt ppm of nitrogen and 30 to 130 wt ppm of oxygen.

In order to characterize the corrosion of a variety of Fe-Cr-Mn alloys, eight specimens were grouped near the top of the loop's hot leg, where the exposure temperatures of these clustered specimens ranged from 485 to 500°C. The remaining coupon positions around the loop were occupied by type 316 stainless steel specimens. Two loop experiments were conducted in this way for total exposure times of 3340 and 3096 h, respectively. The first experiment contained Fe-Cr-Mn specimens provided by H. R. Brager of the Hanford Engineering Development Laboratory (HEDL); in the second series, alloys from HEDL and Oak Ridge National Laboratory (the latter developed by P. J. Maziasz and R. L. Klueh) were exposed. The compositions of these alloys are listed in Table 1.

Results

The weight changes measured for the Fe-Cr-Mn alloys exposed in the two thermal convection loop experiments are shown in Figs. 1 and 2. The steels containing 30 wt % Mn suffered very high weight losses that increased with exposure time. In contrast, the 12 to 20 wt % Mn alloys exhibited a mixture of weight gains and losses that were not always monotonic with time. However, in every case, each 12 to 20 wt % Mn specimen gained weight over approximately the last 2000 h of exposure.

The large number of Fe-Cr-Mn alloys exposed in these experiments precludes inclusion of the microstructural and compositional data for each

specimen (but other data can be found elsewhere [8]). Therefore, results showing the general representative behavior of the alloys are presented. For the 30 wt % Mn alloys, exposure to lithium resulted in the development of rough, porous surfaces on which some "nodules" were also observed (see Fig. 3) Energy dispersive x-ray (EDX) analyses indicated that these nodules were principally chromium and that the underlying corroded surfaces were severely depleted in manganese (to below 3 wt %). In contrast, the corroded surfaces of the 12 to 20 wt % Mn alloys tended to have many more of these chromium-rich nodules. On a few of these specimens, an underlying, porous surface could be observed in gaps between nodule aggregates (see Fig. 4a), while, as shown in Fig. 4b, the nodules completely covered the surfaces of other coupons. Examination of polished cross sections showed that porosity developed on every specimen and that the depth of the porous layer varied among the specimens without any direct relationship to the density of the overlying nodules. Figure 5 shows extremes in the development of these porous layers; it includes microprobe elemental x-ray maps indicating manganese depletion throughout the porous corrosion layers and chromium-rich phases both on the surface and within these altered zones. These observations were confirmed by wavelength dispersive x-ray profiles of the cross sections of selected specimens obtained with the electron microprobe; typical results are shown in Fig. 6 and indicated manganese depletion and surface enrichment in chromium. Compositional data obtained from EDX analyses of the normal and cross sectional surfaces in the scanning electron microscope were consistent with the electron microprobe results.

The location of type 316 stainless steel specimens in the cold leg during the loop experiments allowed the cold zone deposition reactions to also be characterized by weight changes and microstructural analyses. The coldest loop coupon (350°C) gained considerable weight, particularly during the experiment in which the 30 wt % Mn steels were exposed in the hot zone. Numerous large deposits formed at the coldest loop coupon positions (see Fig. 7). EDX analyses showed that such deposits were principally composed of nickel and manganese.

Discussion

The necessity of exposing a range of specimen compositions in a loop of yet another composition precludes an unambiguous interpretation of thermal gradient mass transfer effects because of the introduction of concentration (dissimilar metal) gradients. This point was recognized when the experiments were initially conceived, but as discussed below, some important information about the corrosion of Fe-Cr-Mn alloys by thermally convective lithium was nevertheless gained from these experiments.

The observation of mixed weight gains and losses for the steels containing 12 to 20% Mn indicated a competition between dissolution and weight gain reactions. In agreement with results from experiments in static lithium [2], the present EDX analyses, microprobe imaging, and depth profile data (see Figs. 5 and 6) indicate that the reactions include concentration gradient chromium transport among the specimens and loop wall in the hot zone, a small amount of nickel redistribution to the Fe-Cr-Mn specimens, and preferential dissolution of manganese. Such competing reactions can lead to

a net weight gain if the addition of reacted material due to dissimilar metal mass transfer is greater than that lost by dissolution of manganese and other elements.

Each of the specimens clustered in the 485 to 500°C zone of the lithium loop, including those with significant net weight gains, were found to have corrosion layers characteristic of the type caused by preferential dissolution of an alloy. These layers, containing dark-etching phases or pores are shown in Fig. 5 and bear a strong resemblance to layers on Fe-Ni-Cr steels exposed to lithium [9]. In the present case, the porous layers appear to be associated with the selective leaching of manganese while, for Fe-Cr-Ni systems [9], they are related to preferential depletion of nickel. In the case of the 30 wt % Mn alloys (X75, R77, and R80), this preferential dissolution obviously dominated the corrosion processes and resulted in the large weight losses shown in Fig. 1. For the 12 to 20 wt % Mn specimens, the porous layer was generally deeper and more uniform for the alloys showing net weight losses. Conversely, the Fe-Cr-Mn steel with the largest weight gain after 3096 h (Age 18-18+) showed a very thin dissolution zone, and the one with the next greatest increase in weight (R87) showed a somewhat thicker, but very irregular corrosion layer. Given the trend of the weight change versus exposure time curves (see Figs. 2 and 3) and the observation of many chromium-rich reaction products on top of the dissolution zones (see Figs. 4–6), it appears that, in many cases, manganese depletion makes the principal contribution to the weight change of the Fe-Cr-(12–20 wt %) Mn alloys during the early stages of exposure. Subsequently, chromium

transport and reaction become dominant and lead to weight gains. The presence of materials of different compositions in the hot zone probably exacerbated the latter reactions.

The exact nature of the reaction(s) involving chromium is not known. The starting concentrations of chromium, nitrogen, and carbon (or the concentration ratios of Cr/N and Cr/C) did not correlate with the weight change data or microstructural results. Nevertheless, the chromium reactions may be driven by the relatively high nitrogen concentrations of some of the Fe-Cr-Mn alloys (see Table 1). Reactions between Cr and N and between Li, Cr, and N are possible [5,10,11] and could lead to increased dissolution and/or reaction product formation at specimen surfaces. The significant intergranular penetration observed for some of these alloys in static lithium [4–6] was related to the presence of such reaction products at grain boundaries. In contrast, there was no evidence for intergranular attack of the alloys exposed in the present experiments even though several of the compositions were common to both studies. The reason for such a discrepancy may possibly be attributed to greater dissolution and preferential leaching under the nonisothermal loop conditions. Alternatively, differences in local solution chemistry and/or interstitial transfer gradients between isothermal and thermally convective conditions may explain the absence of grain boundary attack in the present study.

The observation of deposits on type 316 stainless steel specimens in the cold leg (see Fig. 7) and the large measured weight gains for the coldest coupons indicated substantial mass transport occurred during

exposure to lithium. Much of the deposited material was manganese, which came from the hot leg specimens. The source of the nickel in these deposits was the nickel-containing surfaces in the hotter area of the loop.

A quantitative comparison between the corrosion of Fe-Cr-Mn alloys by thermally convective lithium and that of similarly exposed Fe-Cr-Ni steels cannot be made because of the complications arising from hot leg concentration gradients in the present experiments and the relative limited amount of data for the former alloys. However, it is apparent that the Fe-Cr-Mn steels suffer from the same effects of nonisothermal lithium exposure as do nickel-containing austenitic alloys (preferential dissolution, porosity formation, and extensive mass transport of soluble species to cold zone). Indeed, the measured weight losses of the steels containing 30 wt % Mn after 3340 h at 490 to 500°C (217—391 g/m^2) were much greater than that measured for a Fe-Cr-30 wt % Ni alloy exposed for 2832 h at 500°C (28 g/m^2) [12], despite the competing weight gain reaction with chromium. Such Fe-Cr-Mn alloys are clearly not suitable for use in lithium systems at elevated temperature. Furthermore, the 12 to 20 wt % Mn alloys experienced significant degradation despite the low net weight changes and are not expected to be particularly corrosion resistant in thermally convective lithium.

Conclusions

Fe-Cr-Mn alloys containing 30 wt % Mn suffered large weight losses due to mass transfer of manganese. Such steels are clearly not suitable for use in elevated temperature lithium systems.

In Fe-Cr-(12–20 wt %) Mn alloys, competing mechanisms of weight loss resulting from manganese transport and weight gain due to chromium reactions were observed. For these alloys, it appeared that manganese depletion dominated initially, but that it was then offset by chromium reactions that were exacerbated by dissimilar metal gradients in the hot leg. Despite their lower long-term radioactivity, the corrosion of such Fe-Cr-Mn alloys by lithium appears problematical.

References

[1] F.W. Wiffen and R.T. Santoro, in: Proc. Topical Conf. on Ferritic Alloys for Use in Nuclear Energy Technologies, Warrendale, Pa., 1984 (AIME, 1984) pp. 195–200.

[2] V. Coen et al., J. Nucl. Mater. 86&86 (1979) 217–275.

[3] E. Ruedl et al., Material Behavior and Physical Chemistry in Liquid Metal Systems (Plenum, New York, 1982) pp. 97–104.

[4] E. Ruedl et al., J. Nucl. Mater. 110 (1982) 28–36.

[5] E. Ruedl and T. Sasaki, J. Nucl. Mater. 116 (1983) 112–122.

[6] E. Ruedl et al., J. Nucl. Mater. 122&123 (1984) 1247–1251.

[7] P.F. Tortorelli and J.H. DeVan, in: Proc. 3rd Intern. Conf. on Liquid Metal Engineering and Technology, Oxford, 1984 (BNES, London, 1984) pp. 81–88.

[8] P.F. Tortorelli and J.H. DeVan, in: ADIP Semiannual Progress Reports for Periods Ending Sept. 30, 1984; Mar. 31, 1985; Sept. 30, 1985; and Mar. 31, 1986, DOE/ER-0045/13,14,15, and 16 (U.S. Department of Energy, Office of Fusion Energy, 1984–1986).

[9] P.F. Tortorelli and J.H. DeVan, Microstructural Sci. 12 (1985) 215–26.

[10] W.F. Calaway, in: Proc. 2nd Intern. Conf. on Liquid Metal Technology in Energy Production, Richland, Wa., 1980 (U.S. Department of Energy, 1980) pp. 18-8–18-26.

[11] M.G. Barker et al., J. Nucl. Mater. 114 (1983) 143–149.

[12] P.F. Tortorelli and J.H. DeVan, J. Nucl. Mater. 103&104 (1981) 633–638.

Table 1. Compositions of alloys exposed to thermally convective lithium between 500 and 480°C[a]

Alloy	Composition (wt %)[b]						
	Mn	Cr	Ni	C	N	Si	Fe
X75	30	2	0.5	0.1	0.15	0.4	bal
R77	30	2	0.5	0.6	0.15	0.4	bal
R80	30	10	0.5	0.50	0.10	0.4	bal
18-18+	18	18	0.5	0.1	0.4	0.6	bal
Age ı -18+	18[c]	18	0.5	0.1	0.4	0.6	bal
AMCR	17	10	0.7	0.2	0.06	0.6	bal
R88	15	15	0.5	0.3	0.30	0.4	bal
R87	15	15	0.5	0.1	0.1	0.4	bal
NIT-32	12	18	1.5	0.1	0.4	0.6	bal
PCMA-2	17	15	0.01	0.06	0.001	0.04	bal
PCMA-4	19	10	0.01	0.09	0.002	0.02	bal
PCMA-6	14	16	0.01	0.18	0.003	0.02	bal
PCMA-7	19	15	0.01	0.38	0.005	0.02	bal
PCMA-9	18	20	0.01	0.26	0.006	0.03	bal
CN13	1.7	17	14.0	0.05		0.6	bal
316 SS	2	17	10	0.05		0.4	bal

[a]PCMA alloys developed at Oak Ridge National Laboratory; other alloys supplied by Hanford Engineering Development Laboratory.

[b]Analyses provided with alloy material.

[c]Electron beam techniques revealed Mn concentration of 12 wt %. This correction probably applies to the 18-18+ alloy also.

Figure captions

Fig. 1. Weight loss versus time for Fe-Cr-30 wt % Mn alloys exposed to thermally convective lithium. Part of first loop experiment.

Fig. 2. Weight change versus time for Fe-Cr-(12—20 wt %) Mn and Fe-Cr-(12—14 wt %) Ni alloys exposed to thermally convective lithium in (a) first and (b) second loop experiments. ("P" denotes "PCMA".)

Fig. 3. Surface of alloy X75 (30 wt % Mn) after exposure to thermally convective lithium at 495°C for 3340 h.

Fig. 4. Typical surfaces of 12 to 20 wt % Mn alloys exposed to thermally convective lithium for 3096 h. (a) NIT-32, 485°C. (b) R87, 500°C.

Fig. 5. Backscattered electron images (BSI) and elemental x-ray maps of Fe-Cr-Mn alloys exposed to thermally convective lithium for 3096 h. (a) NIT-32, 485°C. (b) Age 18-18+, 490°C.

Fig. 6. Wavelength dispersive x-ray depth profile for PCMA-4 exposed to thermally convective lithium for 3096 h at 485°C.

Fig. 7. Cold leg deposits of Ni-Mn formed on 350°C coupon after 3340 h of exposure of Fe-Cr-(12—30 wt % Mn) alloys in the hot leg of a lithium thermal convection loop.

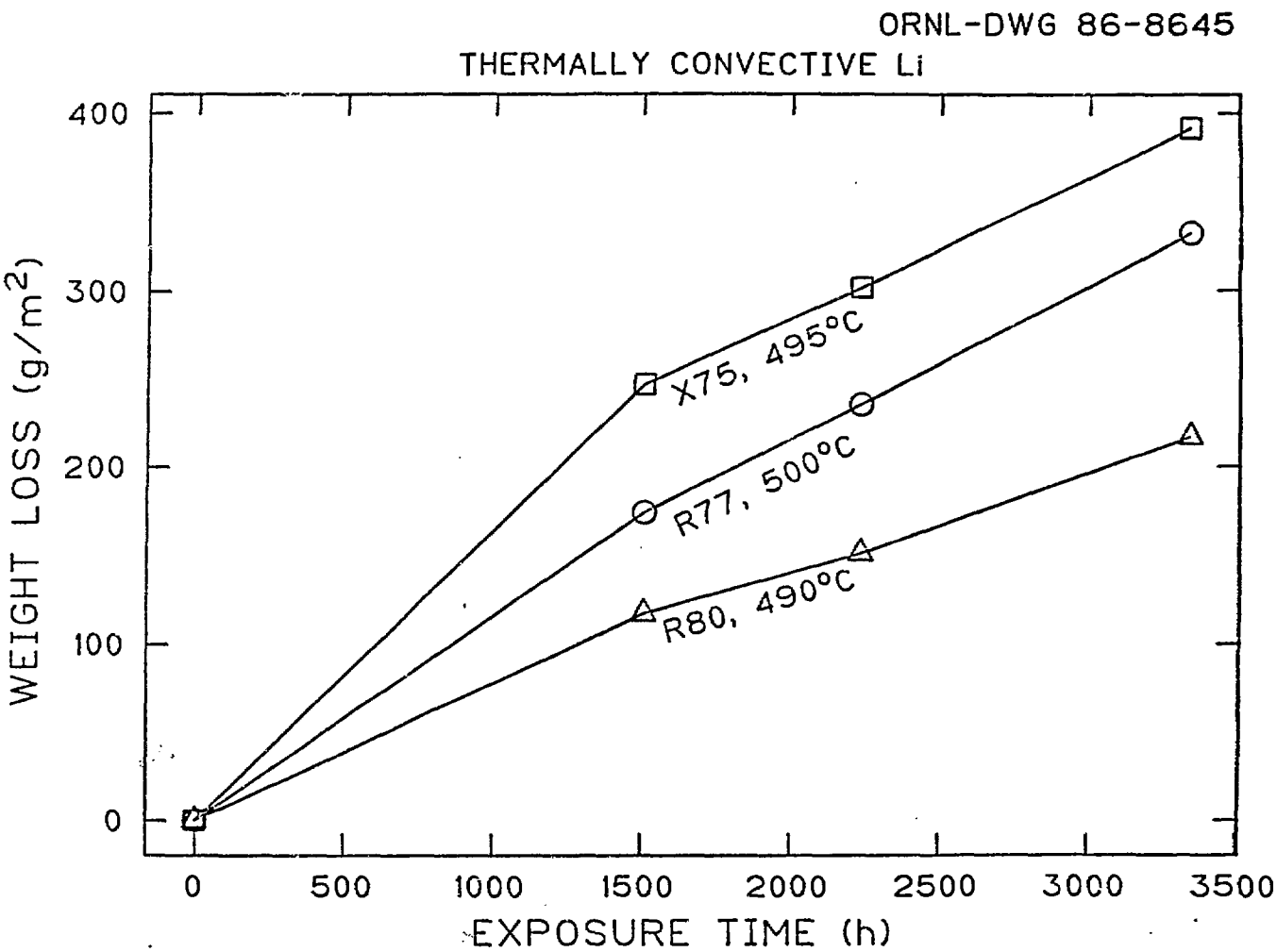
ORNL-DWG 86-8645
THERMALLY CONVECTIVE Li
WEIGHT LOSS (g/m²)
400
300
200
100
0
0
500
1000
1500
2000
2500
3000
3500
EXPOSURE TIME (h)
X75, 495°C
R77, 500°C
R80, 490°C

FIG. 1

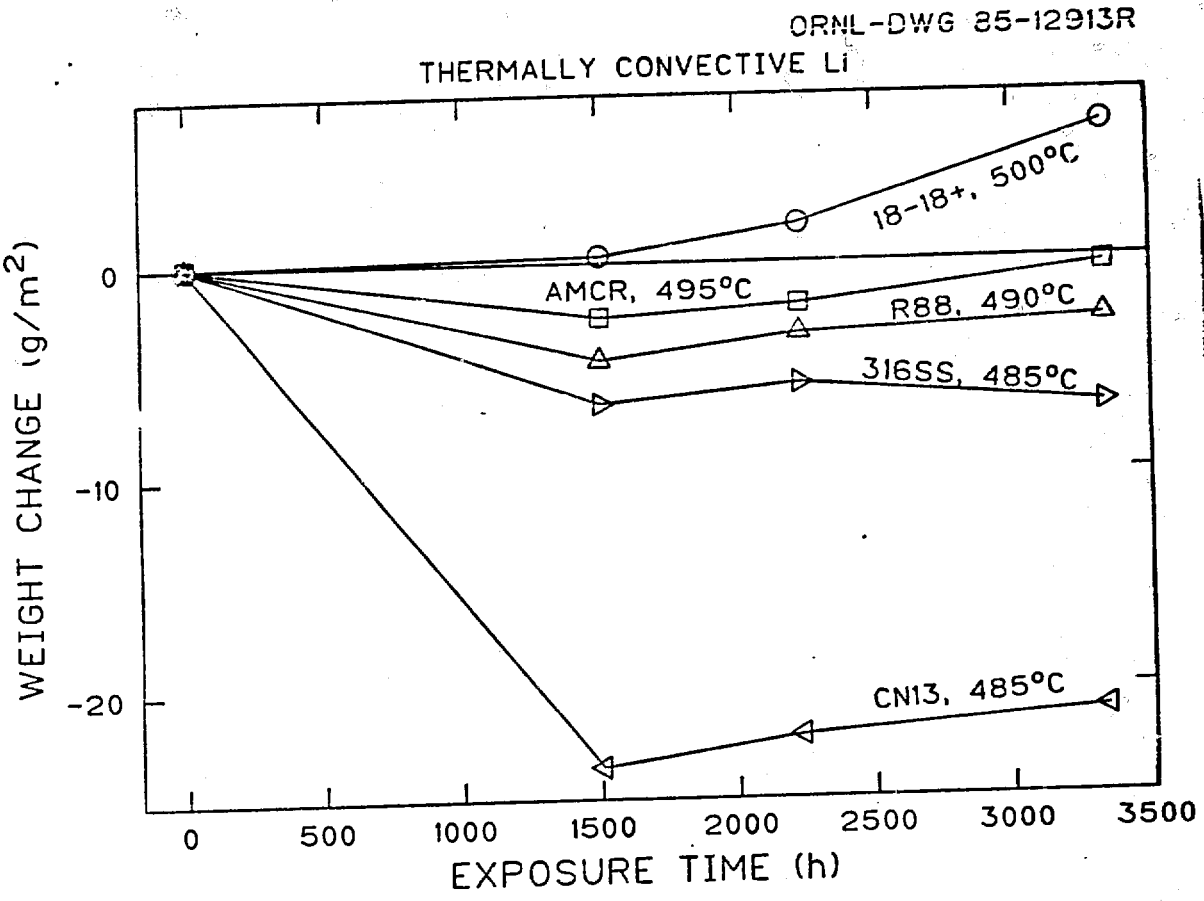
ORNL-DWG 85-12913R
THERMALLY CONVECTIVE Li
18-18+, 500°C
AMCR, 495°C
R88, 490°C
316SS, 485°C
CN13, 485°C
WEIGHT CHANGE (g/m²)
0
-10
-20
0
500
1000
1500
2000
2500
3000
3500
EXPOSURE TIME (h)

(a)

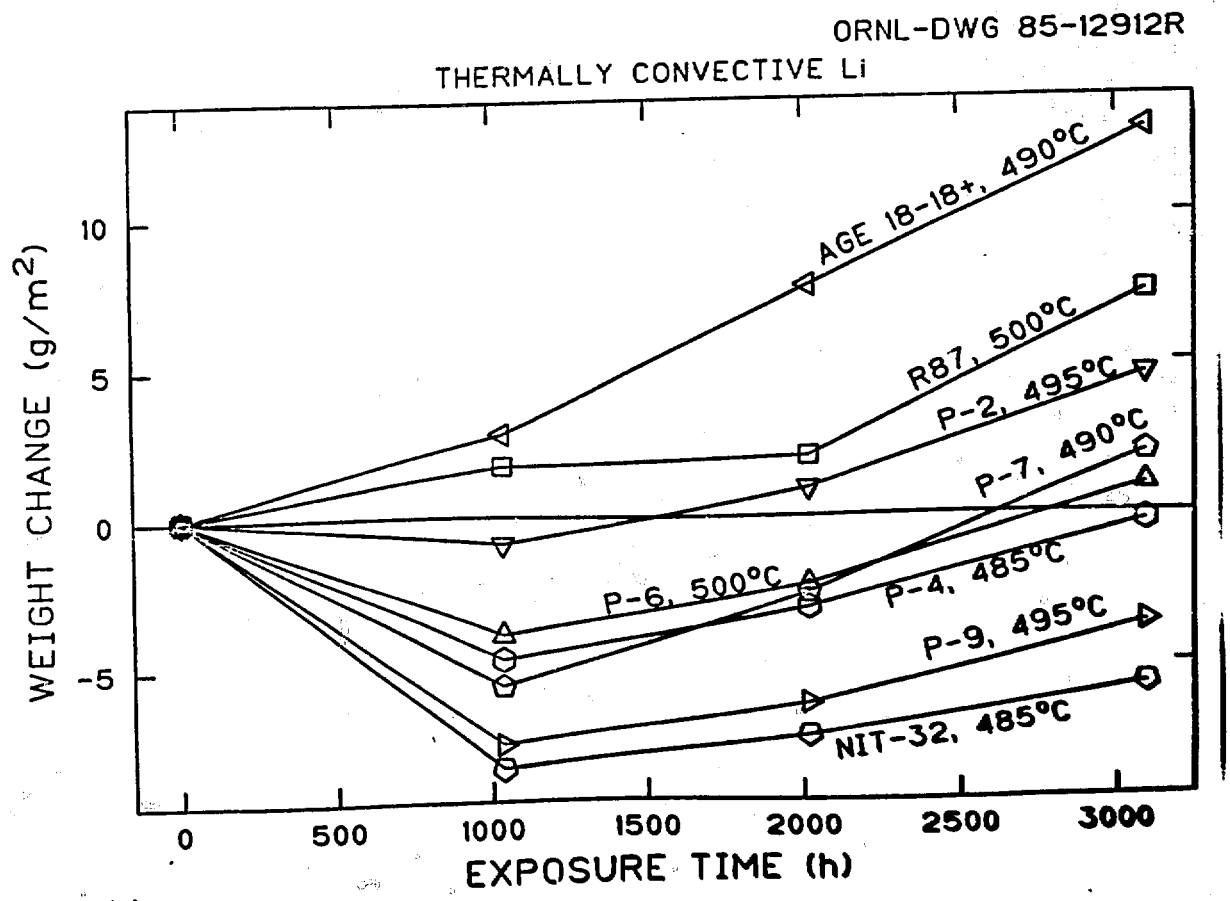
ORNL-DWG 85-12912R
THERMALLY CONVECTIVE Li
AGE 18-18+, 490°C
R87, 500°C
P-2, 495°C
P-7, 490°C
P-6, 500°C
P-4, 485°C
P-9, 495°C
NIT-32, 485°C
WEIGHT CHANGE (g/m²)
10
5
0
-5
0
500
1000
1500
2000
2500
3000
EXPOSURE TIME (h)

(b)

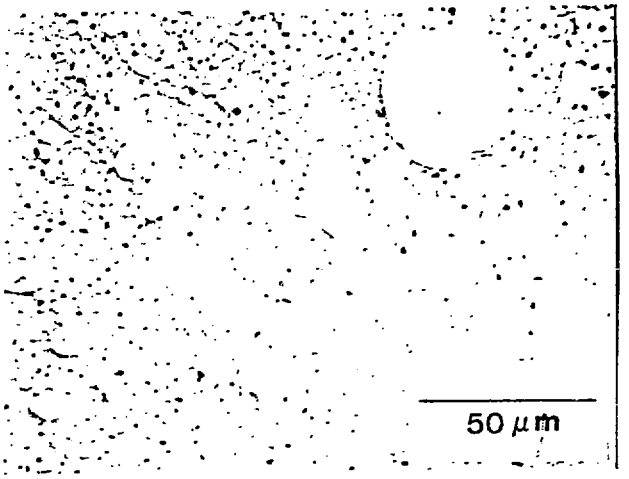

Fig. 3

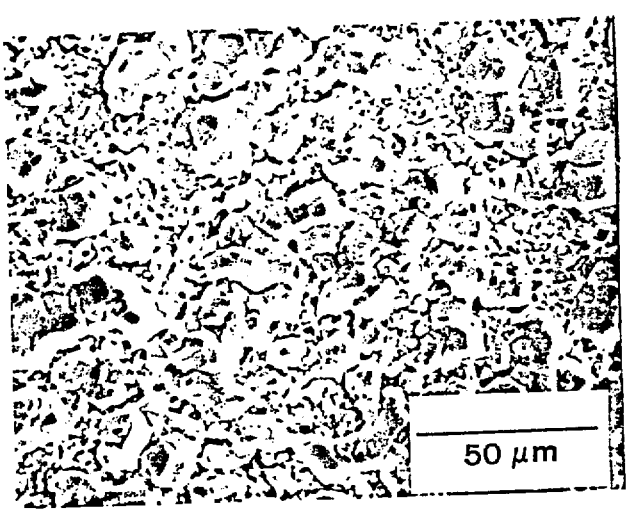

a

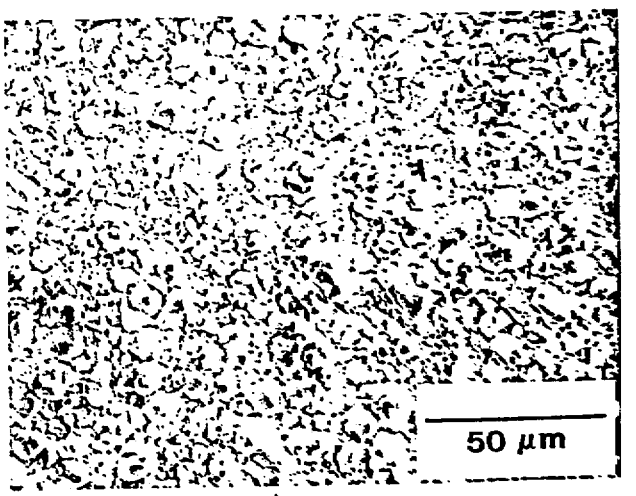

b

Fig. 4

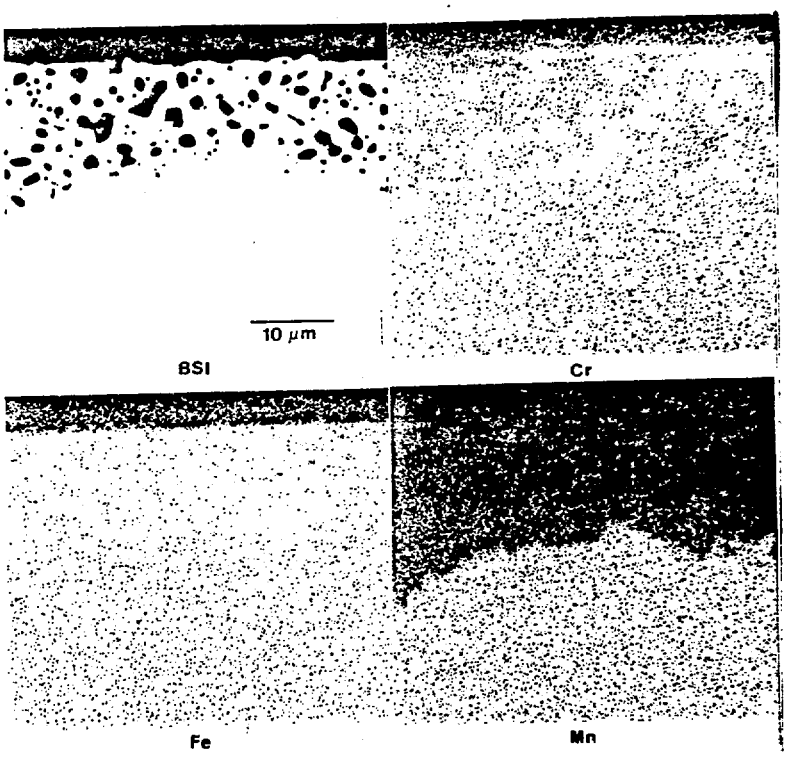

a

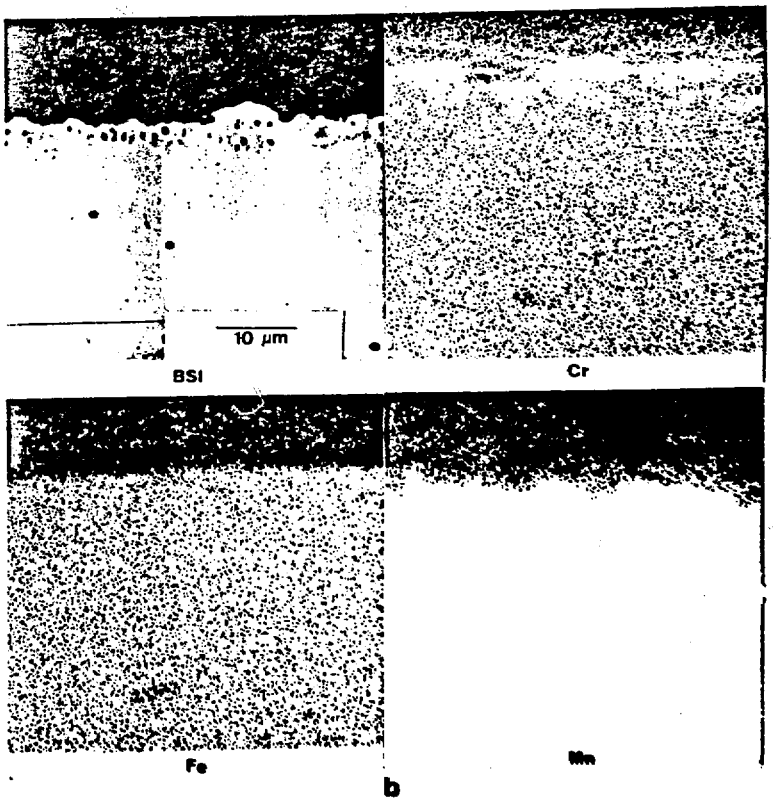

b

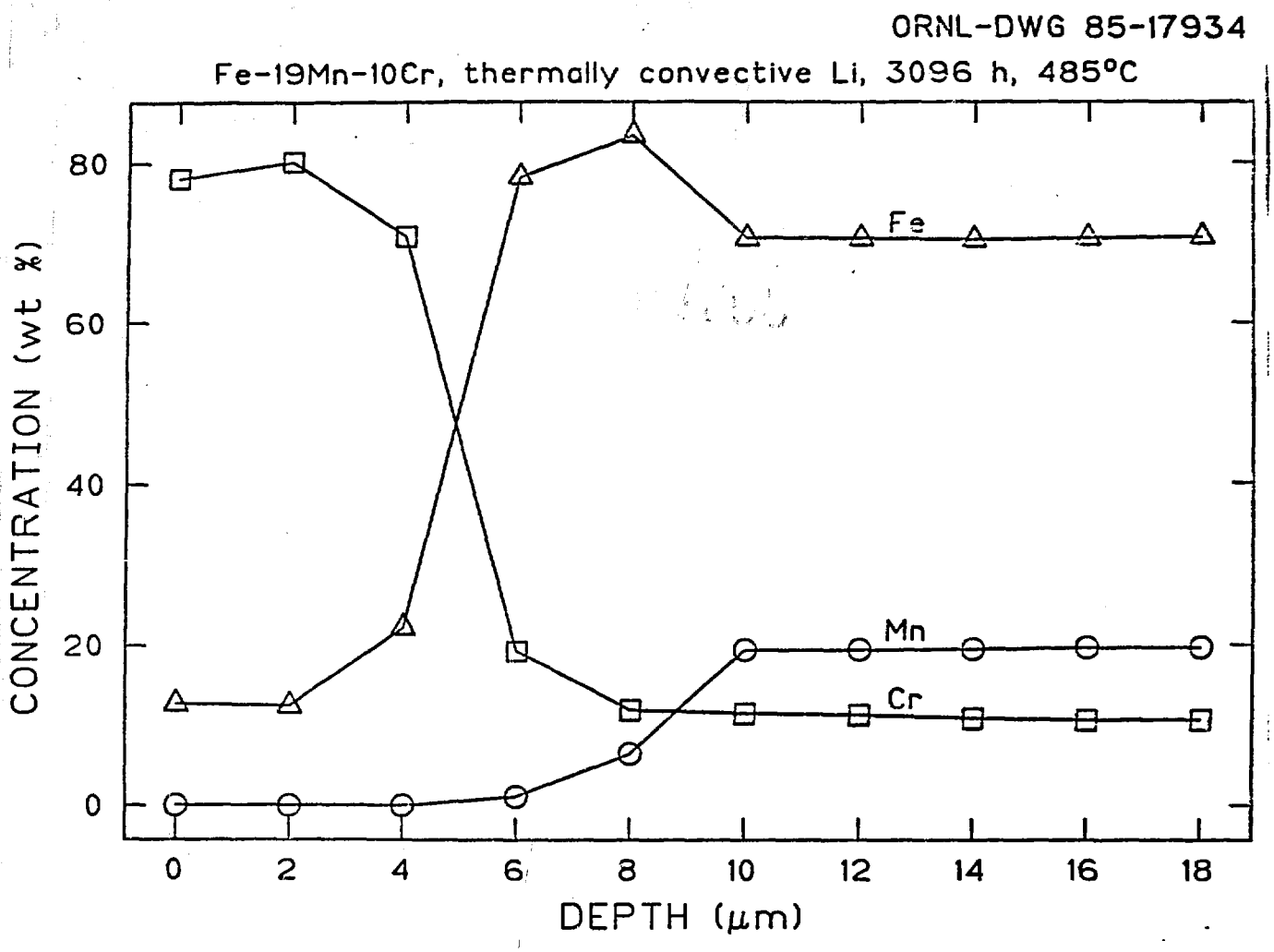
ORNL-DWG 85-17934
Fe-19Mn-10Cr, thermally convective Li, 3096 h, 485°C
CONCENTRATION (wt %)
80
60
40
20
0
Fe
Mn
Cr
0
2
4
6
8
10
12
14
16
18
DEPTH (μm)

FIG. 6

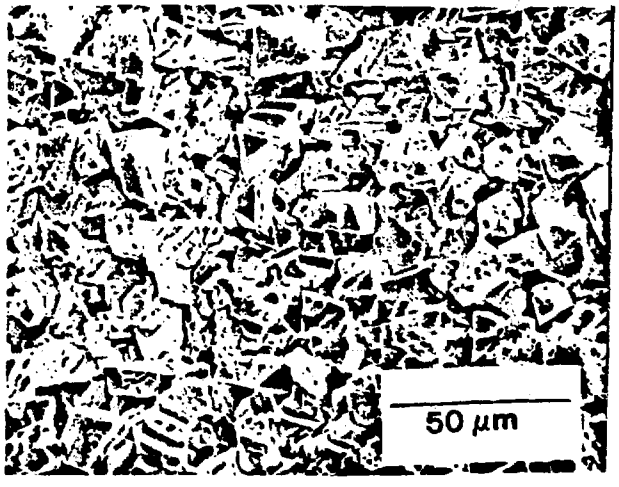
50 μm

Fig. 7